Energy Proceedings
Vol 58, 2025
ISSN 2004-2965

# Real-time Estimation of Surface Downwelling Longwave Radiation from Satellite Imagery for Sky Radiative Cooling Applications

Yuying XIE[1], Mengying LI[1*]

1 Department of Mechanical Engineering, The Hong Kong Polytechnic University

(Corresponding Author: mengying.li@polyu.edu.hk)

**ABSTRACT**

Passive sky radiative cooling systems, which utilize the universe as a natural heat sink, have emerged as a critical technology for providing low-carbon solutions to urban cooling. Surface downwelling longwave radiation (SDLR), originating from the atmosphere, significantly influences the cooling potential of such systems. Therefore, accurately estimating SDLR is pivotal for the design and performance evaluation of these cooling systems. However, real-time SDLR data is generally scarce or lacks accuracy, primarily due to the complex interactions between atmospheric radiation and the inherent variability of clouds. To address this challenge, this work proposes a novel K-means-multilayer perceptron (MLP) model to estimate cloud optical properties and SDLR using high-resolution (5-min, 2-km) geostationary satellite imagery combined with an enhanced two-stream, spectrally resolved radiative model. When validated against one year (2019) of SDLR measurements from the Surface Radiation Budget Network (SURFRAD) across diverse climatic regions in the contiguous United States, the proposed model achieves root mean square error values ranging from 20-25 W/m² across all stations. These findings highlight the capability of this data-driven model to deliver low-latency, accurate estimations of cloud optical properties and SDLR using real-time satellite imagery. The advancement provides promising tools and atmospheric data sources to support the development of advanced sustainable energy systems in urban environment.

**Keywords:** sky radiative cooling, surface downwelling longwave radiation, cloud optical properties, radiative transfer model, remote sensing, deep learning

**NONMENCLATURE**

| | |
|---|---|
| *Abbreviations* | |
| ABI | Advanced Baseline Imager |
| GOES | Geostationary Operational Environmental Satellite |
| LBL | Line-by-line |
| MLP | Multilayer perceptron |
| MBE | Mean bias error |
| RTM | Radiative transfer model |
| RMSE | Root mean squared error |
| SDLR | Surface downwelling longwave radiation |
| SURFRAD | Surface Radiation Budget Network |
| TOA | Top of atmosphere |
| *Symbols* | |
| $b$ | Band number |
| clc | Clear-sky |
| $\theta_z$ | Zenith angle |
| $F^{\uparrow}$ | Upwelling flux |
| $F^{\downarrow}$ | Downwelling flux |

## 1. INTRODUCTION

Rapid urbanization necessitates innovative technologies to regulate the urban thermal environment, particularly to mitigate urban heat island effects. Over the past decade, passive sky radiative cooling systems, which dissipate heat in the form of thermal radiation through the atmospheric window (8 to 13 μm) to the cold universe, have emerged as a vital low-carbon technology for urban cooling [1, 2]. As a technology whose performance heavily depends on atmospheric radiative transfer processes, especially surface downwelling longwave radiation (SDLR), real-time SDLR estimation is crucial for the design and performance evaluation of these systems [3]. However, high-quality, spatiotemporally continuous SDLR estimation methods and corresponding datasets remain scarce or lack-accuracy, primarily due to high cost of sensors and the difficulty of characterizing cloud fields – the major modulators of atmospheric radiative transfer processes.

Previous studies have demonstrated remarkable accuracy in estimating clear-sky SDLR, primarily using physical models [4] and parameterized algorithms [5] that correlate SDLR (or sky emissivity as an alternative

# This is a paper for the 11th Applied Energy Symposium: Low Carbon Cities & Urban Energy Systems (CUE2025), July 18-22, 2024, Kitakyushu, Japan.

form) with atmospheric water vapor content. However, under cloudy-sky conditions, SDLR estimation remains challenging due to the inherent variability of cloud properties and their dynamic nature [6]. Accurate characterization and real-time representation of cloud fields are therefore essential for improving SDLR estimations. Although some efforts have been made to quantify the impact of clouds on SDLR using parameterized schemes based on cloud characteristics [7-9], these approaches are constrained by their simplified representations of cloud optical properties.

To retrieve real-time atmospheric conditions, geostationary weather satellites, such as the Geostationary Operational Environmental Satellite (GOES) [10] and Himawari [11], have emerged as reliable, open-source data sources with high spatiotemporal resolution for real-time top-of-atmosphere upwelling radiation fluxes (Level 1 product). However, a significant gap remains in accurately retrieving cloud properties and downwelling radiative fluxes. This challenge arises primarily from the complex dynamics of clouds and their non-linear interactions with radiation, which result in a complicated mapping between upwelling and downwelling fluxes. Currently, retrieval methods rely primarily on well-established radiative transfer models (RTMs) to infer cloud properties and downwelling fluxes, as those models effectively simulate the intricate interactions between radiation and atmospheric constituents [12]. However, their high computational demands significantly limit the applicability of RTMs for real-time applications.

To address these limitations, this work introduces a novel K-means-MLP method designed to accurately and efficiently estimate high-resolution cloud optical properties and SDLR values from satellite data. The proposed approach integrates a physical RTM with deep learning techniques, enabling real-time evaluation and prediction of the performance of sky radiative cooling technologies and other outdoor energy devices.

## 2. DATA

Two publicly available datasets from 2019 are utilized in this work: (1) remote sensing data from the latest generation of the Geostationary Operational Environmental Satellite (GOES) series (specifically, GOES-16 launched in 2016), and (2) ground-level radiation measurements from the Surface Radiation Budget Network (SURFRAD) sites.

### *2.1 Remote Sensing Data*

The GOES series consists of four satellites equipped with nadir-pointing, solar-pointing, and in situ instruments [13]. This work utilizes multi-band data from the Advanced Baseline Imager (ABI), covering the Contiguous United States. To enable SDLR estimation during both daytime and nighttime, only data from the longwave bands are considered. These bands offer data with a temporal resolution of 5 minutes, and spatial resolution ranging from 0.5 to 2.0 km, as detailed in Table 1. Spectral radiance data from the pixel directly above the ground stations is analyzed.

*Table 1 GOES-R Series ABI Instrument characteristics of longwave channels*

| Band No. | Center wavelength, μm | Full width at half max, μm |
|---|---|---|
| 7 | 3.9 | 3.80–3.99 |
| 8 | 6.2 | 5.79–6.59 |
| 9 | 6.9 | 6.72–7.14 |
| 10 | 7.3 | 7.24–7.43 |
| 11 | 8.4 | 8.23–8.66 |
| 12 | 9.6 | 9.42–9.80 |
| 13 | 10.3 | 10.18–10.48 |
| 14 | 11.2 | 10.82–11.60 |
| 15 | 12.3 | 11.83–12.75 |

### *2.2 Ground-based Measurements*

Ground measurements are collected from seven SURFRAD stations, as shown in Fig.1. These stations include Bondville, Illinois (BON); Fort Peck, Montana (FPK); Goodwin Creek, Mississippi (GWN); Pennsylvania State University, Pennsylvania (PSU); Sioux

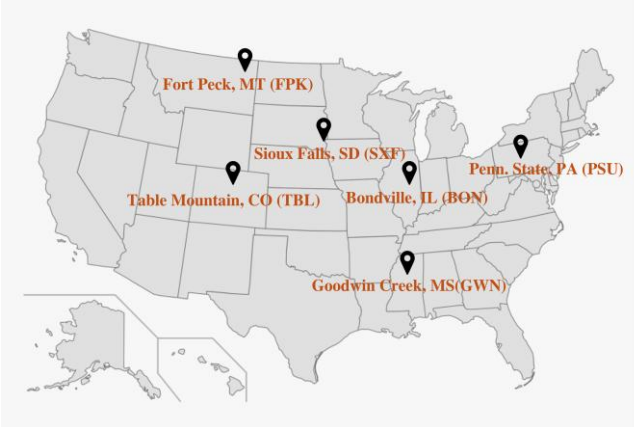


*Fig. 1 Geographic distribution of the SURFRAD stations*

Falls, South Dakota (SXF); and Table Mountain, Boulder, Colorado (TBL). To ensure consistency with satellite data,

all ground-based measurements are converted to standard international units and resampled into 5-minute backward-averaged values.

Daytime and nighttime conditions are classified based on the solar zenith angle $\theta_z$, with daytime defined as $\theta_z \leq 85^\circ$. Additionally, following the clear-sky classification methodology proposed by [14], the daytime data is further categorized into clear-sky and cloudy-sky conditions. Overall, the data from each station is classified into three categories for further analysis: (1) daytime cloudy, (2) daytime all-sky (clear and cloudy), and (3) nighttime all-sky.

## 3. METHODOLOGY

### *3.1 Radiative transfer model*

The line-by-line (LBL) RTM developed by [15] is employed to simulate the atmospheric radiative transfer in the longwave spectrum. The 120 km-thick atmosphere is divided into plane-parallel layers based on pressure, and downwelling and upwelling flux across each layer boundary are calculated using the two-flux approach. Atmospheric gas concentrations, including water vapor, carbon dioxide and others, follow standard Air Force Geophysical Laboratory midlatitude profiles, with real-time adjustments for water vapor based on ground-level temperature and humidity measurements. Absorption coefficients for these gases are obtained from the HITRAN database and are further complemented by the MT_CKD continuum model. The aerosol profile is derived from CALIPSO satellite data, with its optical properties calculated using Mie theory. Similarly, cloud optical properties are modeled using Mie theory, assuming an effective droplet radius of 10 $\mu$m and a variance of 0.1 for the droplet size distribution. The model approximates anisotropic scattering processes as isotropic scattering using the $\delta$-M approximation. Following this scaling, each layer is treated as diffuse and isotropic. The two-flux approach is then applied to recursively compute spectral radiosity and irradiation of each layer by solving the energy balance equation for each layer. Finally, the upwelling and downwelling flux at all the layer boundaries are derived from the radiosity and irradiation results.

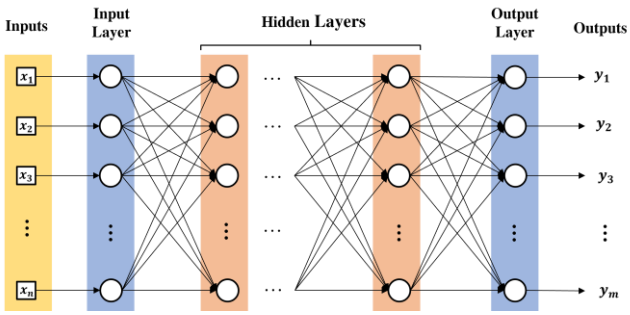


*Fig. 2 Fundamental configuration of MLP*

### *3.2 K-means clustering algorithm*

The K-means algorithm, a well-known unsupervised learning method, has been extensively employed for clustering large datasets [16]. This algorithm partitions a given dataset into $k$ distinct clusters by iteratively converging to a local minimum, ultimately producing compact and well-separated clusters. The K-means algorithm operates in two main phases. In the first phase, $k$ cluster centers are randomly initialized, with the number of clusters $k$ predetermined. Each data point is then assigned to the cluster associated with the nearest cluster center. Once all data points have been assigned to clusters, this phase concludes, yielding an initial clustering of the dataset. In the second phase, the centroids of these clusters are recalculated to serve as new cluster centers. Data points are then reassigned to the cluster with the nearest cluster center, and the centroids of the updated clusters become the next set of cluster centers. This iterative process continues until the difference in cluster assignments between successive iterations becomes negligible or reaches a predefined threshold. The objective to be minimized is,

$$E = \sum_{i=1}^{k} \sum_{x \in C_i} |x - x_i|^2 \quad (1)$$

where $k$ denotes the number of clusters, $x$ denotes a data point, and $x_i$ denotes the centroid of cluster $C_i$.

### *3.3 Multilayer Perceptron classifier*

The multilayer perceptron (MLP) classifier is an advanced feedforward artificial neural network designed to map input vectors to corresponding output vectors [17]. The architecture of an MLP consists of multiple layers, including an input layer, one or more hidden layers, and an output layer, as shown in Fig. 2. This structure forms a fully connected network, where each node in a given layer is connected to all nodes in the adjacent preceding and succeeding layers.

MLPs typically include one or more hidden layers, with each neuron employing a nonlinear activation function. The primary training method for MLPs is the backpropagation algorithm, a widely used supervised learning technique. Backpropagation optimizes the the network's weights by minimizing the error between predicted and actual outputs through gradient descent. This iterative process enables the MLP to generalize effectively and learn from labeled datasets, making it a

powerful tool for solving complex classification problems.

### *3.4 The proposed K-means-MLP model*

In this work, a novel K-means-MLP model is proposed for estimating cloud properties and the corresponding SDLR from satellite images in real-time. The model integrates the powerful learning capability of deep learning techniques with the physical realism of radiative modeling.

Initially, the upwelling fluxes ($F_b^{\uparrow}$) at the top of atmosphere (TOA) are modelled using the LBLRTM under predefined cloud conditions. For each cloudy case, the cloud properties are represented by a cloud vector of length *N*, corresponding to an $N$-layer atmosphere configuration (*N* = 32 in this work). In the cloud vector, a zero value indicates the absence of clouds, while non-zero values correspond to the presence of clouds, with the specific values representing the cloud optical depth (COD, $\tau$). Cloud conditions are classified using the K-means clustering algorithm, which groups cloud vectors into distinct categories. Each cluster represents a unique set of cloud conditions that result to similar upwelling fluxes.

To isolate the effects of clouds from other atmospheric constituents, the upwelling flux at TOA under cloud-free conditions is used to calculate the clear-sky index as follows,

$$k_b^{\uparrow} = F_b^{\uparrow}/F_{b,\mathrm{clc}}^{\uparrow} \tag{2}$$

where $F_b^{\uparrow}$ is the TOA upwelling flux for given cloud optical properties in spectral band $b$, and $F_{b,\mathrm{clc}}^{\uparrow}$ denotes the modeled flux under clear-sky conditions.

Then, the clear-sky indices for all longwave spectral bands serve as input features for a MLP classifier, with the corresponding cloud labels serving as the prediction targets. The MLP classifier consists of two hidden layers,

*Table 2 Parameter setting from Keras tuner optimization results*

| Sky conditions | Parameters | Values |
|---|---|---|
| Daytime | Hidden unit 1 | 64 |
| | Hidden unit 2 | 40 |
| | Learning rate | 0.01 |
| Nighttime | Hidden unit 1 | 56 |
| | Hidden unit 2 | 16 |
| | Learning rate | 0.001 |

and its architecture optimized using the Keras Tuner [18]. The number of units in each hidden layer is tuned between 16 and 64, while the learning rate is tuned as $10^{-x}$. The optimized hyperparameters are summarized in Table 2.

During the inference phase, the TOA upwelling spectral flux $\hat{F}_b^{\uparrow}$ from satellite measurements at time $t$ is used to compute the clear-sky index based on the corresponding modeled clear-sky values. For this computation, the ground-level air temperature and relative humidity measured at the same time are used as LBLRTM inputs. These computed clear-sky indexes are then fed into the trained MLP classifier to estimate the cloud labels. The estimated cloud labels are subsequently converted back into cloud vectors, which represent the retrieved cloud properties at the given time. Using these cloud properties, the SDLR ($F_0^{\downarrow}$) is then calculated with the LBLRTM. The conceptual framework of the proposed model is illustrated in Fig. 3.

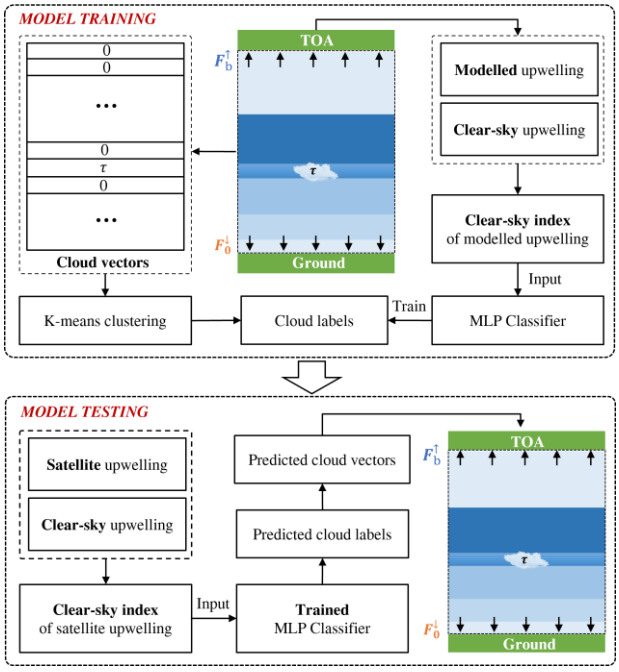


*Fig. 3 Framework of the proposed model*

### 3.5 *Performance evaluation*

The accuracy of SDLR estimation is quantified using root mean squared error (RMSE) and mean bias error (MBE) [19], which are defined as,

$$\mathrm{RMSE} = \sqrt{\frac{1}{N}\sum(f_i - o_i)^2} \tag{3}$$

$$\mathrm{MBE} = \frac{1}{N}\sum(f_i - o_i) \tag{4}$$

where $f_i$ and $o_i$ represent the estimated flux and locally measured flux, respectively, and $N$ is the total number of data points.

## 4. RESULTS AND DISCUSSIONS

The error metrics of the proposed K-means-MLP model for SDLR estimation are presented in Fig. 4. Two benchmark models are included for comparison: (1) our previously developed look-up table-based SCOPE method [20] and (2) a K-means-k-Nearest Neighbor (KNN) model, which uses the KNN algorithm in place of the MLP [21].

The results demonstrate a notable reduction in RMSE for the proposed model, particularly in daytime scenarios (both daytime cloudy and daytime all-sky conditions) across all stations, with RMSE values ranging from 20 W/m² to 25 W/m². Moreover, the MBE values of the proposed model are comparable to those of the SCOPE method and are notably better than those of the K-means-KNN model. These findings highlight the enhanced accuracy of the proposed K-means-MLP model compared to both the physical modelling approach (SCOPE) and the classic machine learning method (K-means-KNN).

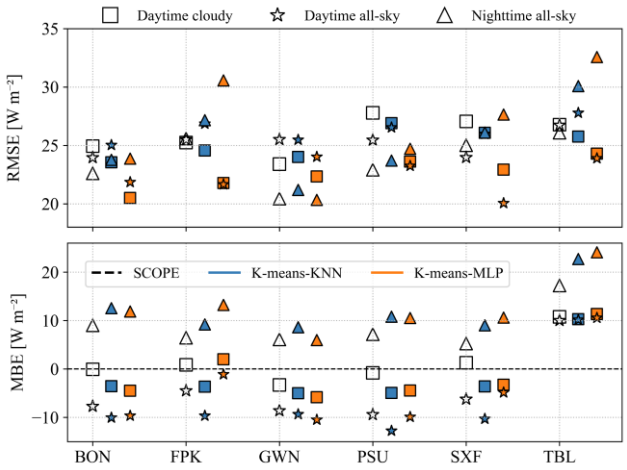


*Fig. 4 Results for the proposed model compared to the benchmark method across stations*

Furthermore, the results emphasize the considerable potential of leveraging deep learning techniques for directly retrieving cloud optical properties from satellite data, enabling more accurate and reliable SDLR estimations.

## 5. CONCLUSIONS

This study proposed a K-means-MLP method for directly retrieving cloud properties from satellite data to enhance the accuracy of SDLR estimations. These advancements have the potential to drive significant progress in innovative urban cooling solutions, particularly in radiative cooling systems, which play a crucial role in the development of low-carbon cities and sustainable energy systems. Future work should focus on exploring state-of-the-art deep learning architectures to achieve further improvements in both accuracy and efficiency in SDLR estimations.


## ACKNOWLEDGEMENT

The authors gratefully acknowledge the support from the Research Grants Council of Hong Kong (Grant numbers C6003-22Y and 25213022).


## REFERENCE


[1] M. Li, Y. Jiang, and C. F. Coimbra, "On the determination of atmospheric longwave irradiance under all-sky conditions," Solar Energy, vol. 144, pp. 40-48, 2017.

[2] W.-L. Shang and Z. Lv, "Low carbon technology for carbon neutrality in sustainable cities: A survey," Sustainable Cities and Society, vol. 92, p. 104489, 2023.

[3] C. F. Coimbra, "Energy meteorology for the evaluation of solar farm thermal impacts on desert habitats," Advances in Atmospheric Sciences, vol. 42, no. 2, pp. 313-326, 2025.

[4] Y. Guo, J. Cheng, and S. Liang, "Comprehensive assessment of parameterization methods for estimating clear-sky surface downward longwave radiation," Theoretical and Applied Climatology, vol. 135, pp. 1045-1058, 2019.

[5] S. Yu et al., "Surface downward longwave radiation estimation from new generation geostationary satellite data," Atmospheric Research, vol. 276, p. 106255, 2022.

[6] Q. Paletta, A. Hu, G. Arbod, and J. Lasenby, "ECLIPSE: Envisioning cloud induced perturbations in solar energy," Applied Energy, vol. 326, p. 119924, 2022.

[7] Y. Zhou and R. D. Cess, "Algorithm development strategies for retrieving the downwelling longwave flux at the Earth's surface," Journal of Geophysical Research: Atmospheres, vol. 106, no. D12, pp. 12477-12488, 2001.

[8] T. Wang, J. Shi, Y. Ma, H. Letu, and X. Li, "All-sky longwave downward radiation from satellite measurements: General parameterizations based on LST, column water vapor and cloud top temperature," ISPRS Journal of Photogrammetry and Remote Sensing, vol. 161, pp. 52-60, 2020.

[9] G. R. Diak, W. L. Bland, J. R. Mecikalski, and M. C. Anderson, "Satellite-based estimates of longwave radiation for agricultural applications,"

Agricultural and Forest Meteorology, vol. 103, no. 4, pp. 349-355, 2000.
[10] J. McCorkel, B. Efremova, J. Hair, M. Andrade, and B. Holben, "GOES-16 ABI solar reflective channel validation for earth science application," Remote Sensing of Environment, vol. 237, p. 111438, 2020.
[11] K. Bessho et al., "An introduction to Himawari-8/9—Japan's new-generation geostationary meteorological satellites," Journal of the Meteorological Society of Japan. Ser. II, vol. 94, no. 2, pp. 151-183, 2016.
[12] S. A. Clough et al., "Atmospheric radiative transfer modeling: A summary of the AER codes," Journal of Quantitative Spectroscopy and Radiative Transfer, vol. 91, no. 2, pp. 233-244, 2005.
[13] T. J. Schmit and M. M. Gunshor, "ABI imagery from the GOES-R series," in The GOES-R Series: Elsevier, 2020, pp. 23-34.
[14] R. H. Inman, J. G. Edson, and C. F. Coimbra, "Impact of local broadband turbidity estimation on forecasting of clear sky direct normal irradiance," Solar Energy, vol. 117, pp. 125-138, 2015.
[15] M. Li, Z. Liao, and C. F. Coimbra, "Spectral model for clear sky atmospheric longwave radiation," Journal of Quantitative Spectroscopy and Radiative Transfer, vol. 209, pp. 196-211, 2018.
[16] S. Na, L. Xumin, and G. Yong, "Research on k-means clustering algorithm: An improved k-means clustering algorithm," in 2010 Third International Symposium on intelligent information technology and security informatics, 2010: Ieee, pp. 63-67.
[17] T. Windeatt, "Accuracy/diversity and ensemble MLP classifier design," IEEE Transactions on Neural Networks, vol. 17, no. 5, pp. 1194-1211, 2006.
[18] S. Joshi, J. A. Owens, S. Shah, and T. Munasinghe, "Analysis of preprocessing techniques, Keras tuner, and transfer learning on cloud street image data," in 2021 IEEE International Conference on Big Data (Big Data), 2021: IEEE, pp. 4165-4168.
[19] D. Chakraborty and H. Elzarka, "Performance testing of energy models: are we using the right statistical metrics?," Journal of Building Performance Simulation, vol. 11, no. 4, pp. 433-448, 2018.
[20] D. P. Larson, M. Li, and C. F. Coimbra, "SCOPE: Spectral cloud optical property estimation using real-time GOES-R longwave imagery," Journal of Renewable and Sustainable Energy, vol. 12, no. 2, 2020.
[21] G. Guo, H. Wang, D. Bell, and Y. Bi, "KNN Model-Based Approach in Classification," 2004.